P2.38   QUANTIZATION OF FAR FIELD DIFFRACTION AND FOCAL PLANE MISALIGNMENT EFFECTS ON SIMULATED GIFTS DATA FROM THE IHOP FIELD PROGRAM

Erik R. Olson[*], Robert O. Knuteson, Hank E. Revercomb, Jun Li, Hung-Lung Huang

Cooperative Institute for Meteorological Satellite Studies (CIMSS)
University of Wisconsin-Madison
Madison, WI 53706

The Geosynchronous Imaging Fourier Transform Spectrometer (GIFTS) and the Hyperspectral Environmental Suite (HES) instruments are geostationary infrared spectrometers. Geostationary orbit provides observations with very good time resolution, but also increases the effect of diffraction. There can be significant differences in emitted radiances due to clouds and changes in surface characteristics. High, thick clouds in particular are much cooler than clear areas. Diffraction causes radiation that originates from cloudy areas outside of the detector field of view to contaminate the clear pixels. GIFTS will also have two detector arrays on different focal planes, which may not be perfectly aligned. This can cause spatial misalignment between the data for the two spectral regions.

High spatial resolution numerical models run at the University of Wisconsin - Cooperative Institute for Meteorological Satellite Studies (UW-CIMSS) provide data for examining the diffraction and misalignment effects. The model data represents a variable cloud case during the IHOP field experiment at 1.3-km resolution. This paper outlines the production of high spatial resolution simulated data, characterization of the far field diffraction effects on radiances, and analysis of misalignment effects on temperature and moisture profile retrievals.

1. INTRODUCTION

Satellite remote sensing instruments typically have a listed field of view (FOV) size, which is a concise way to numerically describe the angular resolution and diffraction inherent in the instrument design. It is convenient to think about the data as the signal coming from non-overlapping FOVs of a certain spatial resolution, but in reality the energy that reaches the detector may come from a very wide FOV. The contributions from sources outside the listed FOV radius are usually small, but need to be quantified to understand when diffraction effects are important. This paper models the diffraction for the GIFTS instrument and demonstrates its effect on brightness temperatures.

The optical point spread function (PSF) for a diffraction limited telescope can be represented by the following formula (Personal Communication, Roy Esplin, Space Dynamics Laboratory Utah State University, July, 2000).

$$\frac{1}{1-\varepsilon}\left\{\left(\frac{2\text{Bes}[1,\pi rd/\lambda h]}{\pi rd/\lambda h}\right)-\left(\frac{2\varepsilon^2\text{Bes}[1,\pi\varepsilon rd/\lambda h]}{\pi\varepsilon rd/\lambda h}\right)\right\}^2$$

Where λ is the wavelength, d is the telescope diameter, ε is the central obscuration diameter ratio, r is the radial distance from the FOV center to the edge, and h is the altitude of the instrument orbit. A plot of this function shows that the contribution to the detector signal drops off rapidly with distance from the center of the FOV, but the total contribution from an area outside a specific radius can be significant due to the r^2 dependence.

* *Corresponding author address*: Erik Olson, 1225 W. Dayton St., University of Wisconsin-Madison, Madison, WI 53706; erik.olson@ssec.wisc.edu.
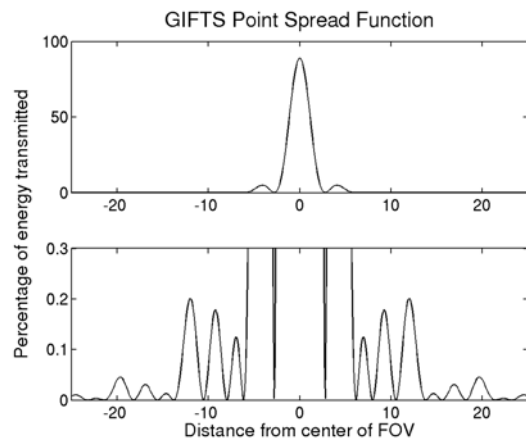
Figure 1. GIFTS point spread function in both full scale and expanded to lobes near 10 kilometers.
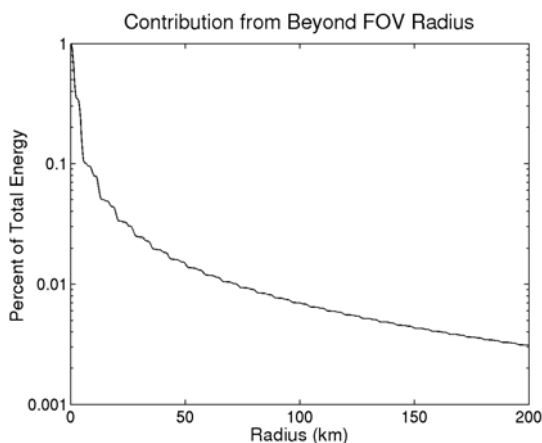

Figure 2. Contribution of the total energy from outside a specified FOV radius.

The first figure shows that there are contribution lobes near a radius of four kilometers where nearly five percent of the energy is diffracted into the detector. The lower axis is just an expanded scale to show that even at 12 kilometers almost 0.2 percent of the energy is diffracted. Figure 2 shows the fraction of total energy that is contributed from outside a given radius. Total energy is defined as the radiance within 1000 km of the FOV center point. The exponential scale highlights the slow trailing off of energy contribution at large radii.

2. DIFFRACTION OF GIFTS DATA

GIFTS simulated data was created at 1.33-km resolution for the study of diffraction and misalignment effects. The MM5 model was used to recreate the atmospheric conditions during the International H_2O Project (IHOP). Top of the atmosphere radiances at 1.33-km resolution are then produced by the GIFTS fast model (Huang et al. 2004). A 4-km resolution control case was produced by averaging a 3 by 3 array of these radiances. Figure 3 shows the control case at 788 cm^{-1} and figure 4 shows the location of the cloudy areas. This wavenumber region is the most susceptible part of the GIFTS spectra to problems with diffraction because it has a combination of longer wavelength (greater diffraction) and low atmospheric absorption (large temperature gradients).
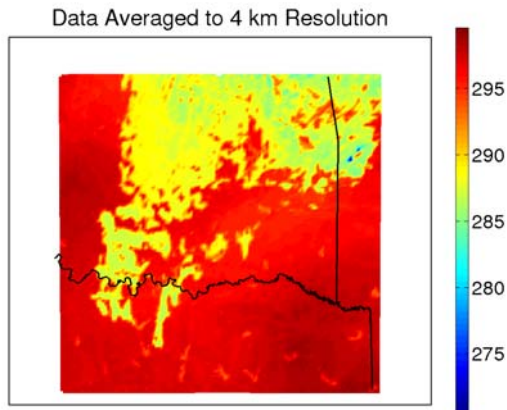

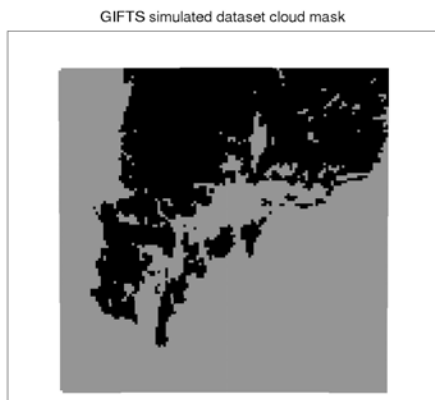Figure 3. High spatial resolution simulated data that has been averaged to the 4 kilometers.

Figure 4. Cloud mask showing cloudy areas in black.

The effect of neighboring scenes was calculated for two different point spread function distances. The first set of calculations is referred to as the near field diffraction effect and is a convolution of the point spread function over an 11 by 11 array of 1.33-km simulated data points. This leads to a near field cutoff of 14.6 km. These results are then averaged over the listed 4-km resolution of the GIFTS instrument. Figure 5a shows the near field diffraction effects minus the averaged control case. Results show the largest differences are near cloud boundaries where the brightness temperature changes are most abrupt.
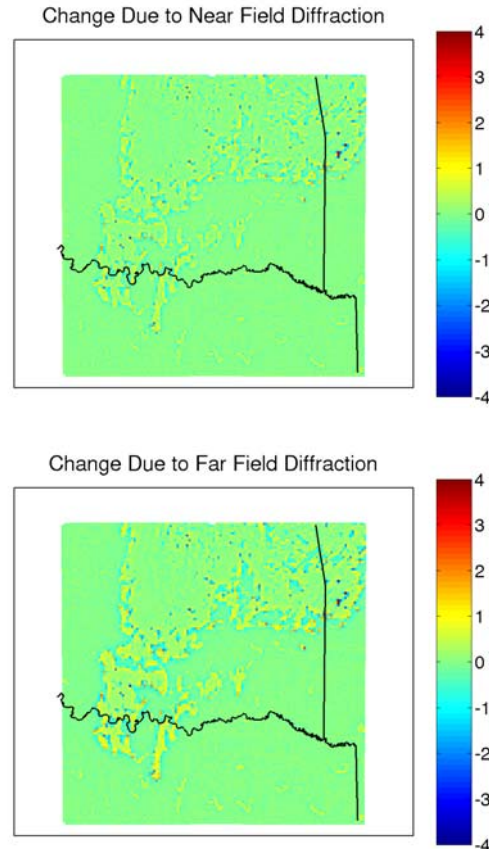

Figure 5. Near and far field diffraction effect on brightness temperatures at 788 cm^{-1}.

The second set of calculations is for the far field diffraction effects. Here the point spread function was convolved with a 259 by 259 array of 1.33-km data, so the far field diffraction covers a 344 kilometer wide area. Since the simulated dataset only contains 384 by 384 points, 128 points in each direction were mirrored beyond the original data to increase the array size. Again the convolution results were averaged to 4-km resolution. The changes due to the far field effects are shown in Figure 5b. The results are very similar to the near field effects with the magnitude of the differences being slightly larger. The same calculations were performed for 735 cm^{-1}. As expected the diffraction

effects are an order of magnitude smaller due to smaller brightness temperature gradients due to significant atmospheric absorption.
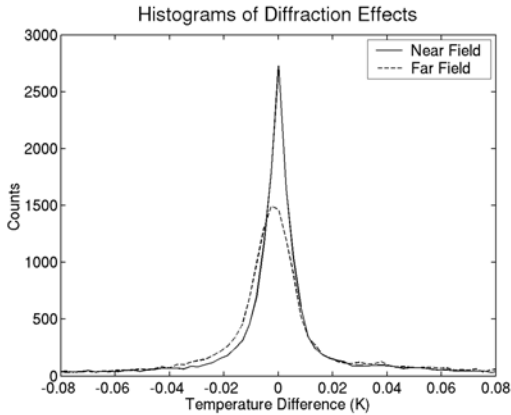

Figure 6. Histograms of the brightness temperature change due to near and far field diffraction effects.

The histogram of the radiance differences for the near and far field cases shows that the far field diffraction has fewer pixels with almost zero brightness temperature changes. The slight negative skew in the far field histogram is due to a small number of very cold ice cloud pixels affecting a large number of warmer pixels.

3. APPLICATION TO REAL DATA

To examine the effect of diffraction on real data, the GIFTS point spread function was applied to a sample dataset from the MODIS Airborne Simulator (MAS). The point spread function was generated at the MAS resolution and applied to the data over a 13-km by 13-km box. The results were then averaged to the nominal GIFTS resolution of 4 km. Figure 7 shows that the most of the differences for the longwave window channels are less than 0.2 degrees with most of the larger changes where large temperature gradients exist.
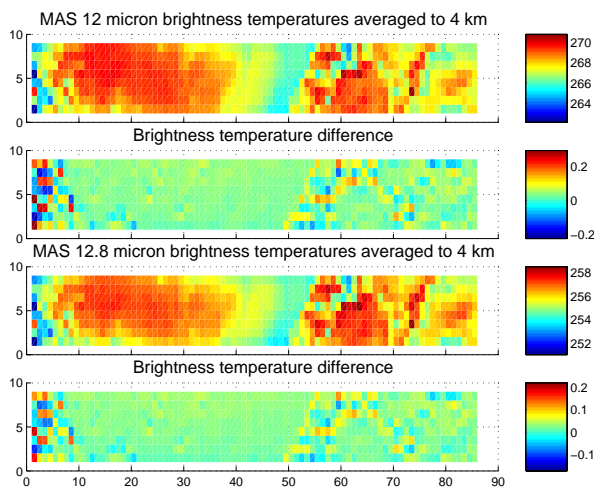

Figure 7. Diffraction results for MAS data.

4. MISALIGNMENT EFFECTS

The GIFTS instruments uses two focal planes to cover different regions of the spectrum. Small errors in the alignment of the focal planes will cause the field of view for the two bands to be slightly different. This can create problems for algorithms like the temperature and water vapor retrievals (Huang et al. 2004), which use data from both spectral regions. Figure 8a shows how the misalignment between the two focal planes of 1.3 kilometers affects the retrieved temperatures. To simulate the misalignment, the short–midwave focal plane data is shifted a variable amount to the left. These shifts are either the distance of one (1.3 km), two (2.7 km), or three (4 km) high resolution pixels. The results are then either averaged to a four kilometer FOV or if diffraction effects are to be applied, the data is convolved with the point spread function before being averaged. Figure 8b shows the difference in retrieved temperatures between the case where the near field diffraction and a 1.3 kilometer misalignment was applied and the case where neither was applied. Differences for cloud covered areas are always zero since the retrievals are not run on areas that are specified as cloudy. In the
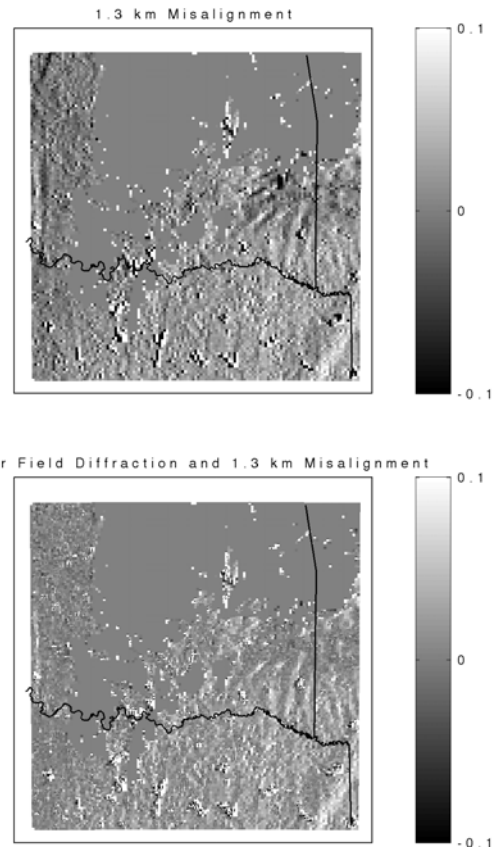

Figure 8. Differences in retrieved 850 MB temperatures due to a) 1.3 kilometer misalignment and b) both the near field diffraction and single 1.3 kilometer pixel misalignment.

undiffracted case, edge effects in the East – West cloud direction are obvious even with a misalignment of 1.3 kilometers.

The errors in the retrievals vary for different levels in the atmosphere. The rms errors in the temperature retrievals show a systematic increase in error as the misalignment between the focal planes increases and a general increase in errors near the surface. It is interesting to note that lowest error case is where the diffraction effect errors cancel out some of the errors due to misalignment.
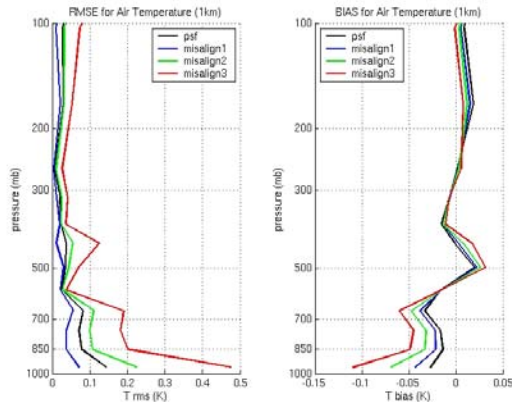

Figure 9. Temperature retrieval biases and errors.

The following histograms show the distribution of changes in the 850 Mb retrieved temperature due to the addition of diffraction and misalignment. The shift in the histograms towards the positive direction is because the test data has a greater number of positive gradients from East to West. In the case where both effects were applied (right panel), the 2.7 km and 4 km shift cases are dominated by the misalignment effects, while the 1.3 km shift case looks more like the diffraction only case.
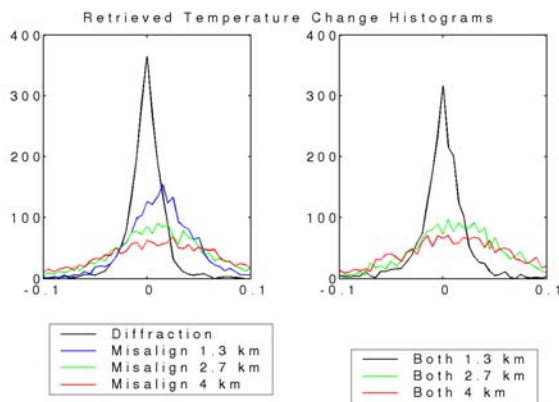

Figure 10. The changes in the retrieved temperatures for a) the near field diffraction only case and the misalignment only cases and b) the cases with both diffraction and misalignment.

For the water vapor retrievals, the errors exhibit the same behavior of a minimum at small misalignments

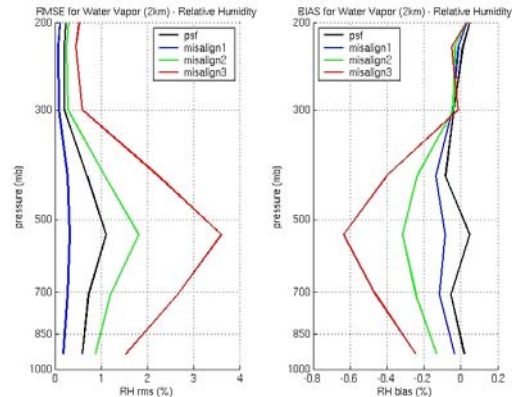followed by an increase in errors as the amount of misalignment becomes greater.

Figure 11. Water vapor retrieval biases and errors.

5. CONCLUSIONS

The effects of diffraction and misalignment are the greatest along regions of large brightness temperature gradients. Algorithms that require an uncontaminated clear FOV should avoid regions close to areas with high gradients of temperature or radiance. This preliminary study indicates that the diffraction effects cause a smearing along cloud boundaries where a small misalignment between the two focal planes is most noticeable. This smearing could mitigate the effects of the misalignment and reduce the accuracy threshold needed for focal plane alignment.

6. REFERENCES

Born, M., E. Wolf, 1980: *Principles of Optics, Electromagnetic Theory of Propagation Interference and Diffraction of Light,* Sixth Edition, Pergamon Press, 416pp.

Huang, H-L., J. Li, E. Weisz, K. Baggett, J. E. Davies, J. R. Mecikalski, B. Huang, C. S. Velden, R. Dengel, S. A. Ackerman, E. R. Olson, R. O. Knuteson, D. Tobin, L. Moy, D. J. Posselt, H. E. Revercomb, and W. L. Smith, 2004: Infrared hyperspectral sounding modeling and processing, 20th Conference on IIPS, 84th AMS Annual Meeting, 11-15 January 2004, Seattle, WA. Published by the American Meteorological Society, Boston, Mass.

Otkin, Jason A., Derek J. Posselt, Erik R. Olson, James E. Davies, Wayne F. Feltz, Robert O. Knuteson, and John R. Mecikalski, 2004: Generation of simulated top of atmosphere radiance datasets for GIFTS/HES algorithm development, 20th Conference on IIPS, 84th AMS Annual Meeting, 11-15 January 2004, Seattle, WA. Published by the American Meteorological Society, Boston, Mass.